Archives of Hydro-Engineering and Environmental Mechanics
Vol. 49 (2002), No. 1, pp. 83–105

Reverse Flow Routing Problem Solved by the Space-Time Conservation Method

Katarzyna Weinerowska

Technical University of Gdańsk, Faculty of Hydro and Environmental Engineering
ul. Narutowicza 11/12, 80-952 Gdańsk, Poland; e-mail: kwein@pg.gda.pl

(Received November 16, 2001; revised February 11, 2002)

Abstract

In the paper, the problem of reverse flow routing (RFR) is examined. The case of gradually varied unsteady flow in an open channel described by the Saint Venant system of equations is considered. The specific difficulties connected with solving the inverse problem are studied and the efficient solution algorithm, based on Space-Time Conservation Method (STC) is presented. The most important features of the proposed scheme are local and global mass conservation and high accuracy, that are of special importance in the case of the reverse flow routing problem. Additionally, the distinguishing feature of the scheme is space and time unification and treating them on the same footing. The way of constructing the computational grid and achieving the final approximation formulas are described in detail. Stability and accuracy analysis, and the numerical examples confirming the good features of the scheme, are developed. Good conformity between the results obtained and required is observed.

1. Introduction

One of the basic problems, which is the starting point of investigating different aspects of open channel hydraulics, is that of unsteady gradually varied flow. Such flow arises as the effect of the forced slow changes of the flow variables (e.g. discharge, water stage etc) and is the common form of the water movement in open channels.

Usually, for most cases of such flow, a sufficiently accurate mathematical description of the phenomenon is achieved by using the system of equations presented in 1871 by Barré de Saint-Venant, which may be written as (Cunge et al. 1980)

$$\frac{\partial A}{\partial t} + \frac{\partial Q}{\partial x} = 0, \tag{1a}$$

$$\frac{\partial Q}{\partial t} + \frac{\partial}{\partial x}\left(\frac{Q^2}{A}\right) + gA\frac{\partial H}{\partial x} + gA\left(S_f - S_o\right) = 0, \tag{1b}$$

where Q is discharge, H – water depth, A – wetted cross-sectional area, S_f – friction slope, S_0 – channel bottom slope, g – acceleration due to gravity, x characterizes longitudinal distance and t time. The 1D model presented is often called the dynamic wave model. The system of partial differential equations given above is of the hyperbolic type (Cunge et al. 1980, Szymkiewicz 2000), and has two families of real characteristics.

Modeling of the gradually varied unsteady flow in open channels is usually connected with solving classical initial – boundary (also called "mixed") problems for the Saint-Venant equation system. Such approach represents so-called direct problems. It enables calculation of the functions describing discharge and water stage changes in time in the considered channel reach, for the imposed changes of these variables in the upstream and/or downstream ends. The problem has been widely analyzed and commonly applied in various practical cases, hence it can be stated that it is well recognized and described, not only as regards the rules governing its proper formulation, but also the methods of solution. Formally, such an approach is connected with integrating the equation system (1a, b) in the increasing time direction.

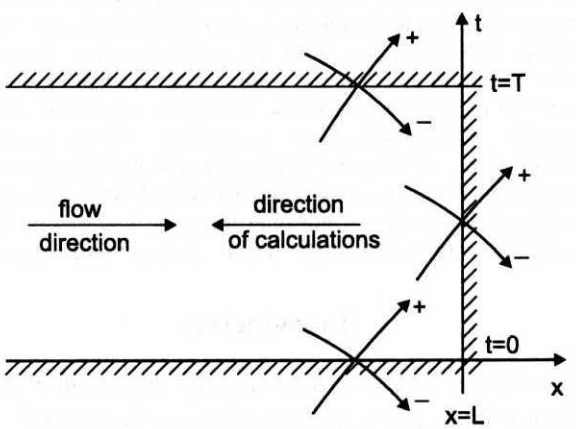

Fig. 1. Solution domain and structure of the characteristics in the reverse flow routing problem

However, the problem mentioned above is not the only one that may be formulated for the system of equations (1a, b) (Eli et al. 1974, Szymkiewicz 2000, Weinerowska 2001). From the practical point of view, there is also another interesting and important case that may be posed for this system of equations. It is connected with calculations in decreasing x direction (Fig. 1). Solving such a problem enables us to obtain $Q_0(t)$ and $h_0(t)$ functions, representing discharge and water stage changes in the upstream cross-section, on the basis of known conditions of flow in the downstream cross-section. Such an approach is called reverse flow routing (RFR) and it is formally an example of the inverse problems in open channel hydraulics. The RFR problem is of considerable practical value,

e.g. in the case of flow controlling, in water resources systems management, when it is important to predict or determine the mode of operation at an upstream point, in order to obtain the desired flow conditions downstream.

Contrary to the classical initial-boundary problem, there is still no successful and detailed recognition of the RFR problem. As the result of the first analysis (e.g. Eli et al. 1974, Cunge et al. 1980) the problem was described as ill-posed, at least for non-linear equations of the hyperbolic type. Achieving its reasonable solution was considered to be possible only in particular cases, when several conditions are satisfied, such as negligibly small friction, short length of the channel and the non-linearity of the advective velocity term not strong (Cunge et al. 1980). Even then, Cunge found it possible to solve the problem only if the method of characteristics was used. Eli (Eli et al. 1974) presented the results of solving the inverse problems for Saint-Venant equations using the implicit differential scheme. Further analysis (Szymkiewicz 1993, Szymkiewicz 1996) proved that the problem can be properly posed if formulated for subcritical flow and provided that an additional set of information at the domain borders is correctly imposed, which enables achievement of the unique solution.

The conditions of proper formulation of the problem can be established on the grounds of the analyses of the characteristics. As presented by Szymkiewicz (1993), the system of equations (1a, b) has two families of characteristics defined as

$$\frac{dt}{dx} = \frac{1}{U + \sqrt{gH}}, \quad \frac{dt}{dx} = \frac{1}{U - \sqrt{gH}}. \tag{2a, b}$$

The slopes of the characteristic curves in the RFR problem are the inverse of those referred in the classical initial-boundary flow routing problem.

The families of the characteristics (2a) and (2b) are of opposite signs where $\sqrt{gH} > U$, which refers to the case of subcritical flow. As the equal number of characteristics of both signs is the condition of invertibility of the flow routing problem (Godunow 1975), the subcritical flow is the only situation in which the proper formulation of the RFR problem is possible. Moreover, the next requirement of this proper posedness is to impose at each boundary of the solution domain (Fig. 1) one boundary condition for every characteristic line leaving the solution domain through this boundary (Godunow 1975). Thus

- two conditions at the boundary $x = L$, (downstream boundary conditions) — e.g. $U(x = L, t) = U_L(t)$ and $H(x = L, t) = H_L(t)$ for $0 \leq t \leq T$
- one condition at the boundary $t = 0$ (initial boundary condition) — e.g. $H(x, t = 0) = H_0(x)$ for $x \leq L$
- one condition at the boundary $t = T$ (final boundary condition) — e.g. $H(x, t = T) = H_T(x)$ for $x \leq L$

must be imposed. The proper specification of the initial and boundary conditions is essential to obtain the unique solution.

As for the direct problem, it is necessary to apply numerical methods in order to solve the RFR problem. The method of characteristics, suggested by Cunge (1980), is – because of its complexity – rather unwieldy. The application of the finite difference method schemes in such cases is much more convenient, relatively easy and it enables one to obtain a solution of good quality. The effective algorithm of solving the reverse flow routing problem by applying the implicit four-point scheme, was presented by Szymkiewicz (1993, 1996, 2000). Unfortunately, even when the conditions of the proper formulation are satisfied, numerical solution of the problem is not always successful. In some cases the solution may suffer from considerable numerical errors arising during calculations. For the RFR problem this question is of particular importance, as - running the calculations backwards, in the opposite direction to the flow – it is necessary to reconstruct the rising gradients of the dependent flow variables. Applying finite differential dissipative or dispersive schemes causes distortions such as unphysical oscillations or the excessive smoothing of the solution. That is why, in the case of inverse problems, special attention must be paid to the choice of the solution method. Because of this, it is worth searching for effective algorithms to solve the problem. In this paper the application of the Space-Time Conservation (STC) Method is proposed.

The relatively new approach presented by Chang (1995), different from those traditionally described in literature (e.g. Potter 1977, Cunge et al. 1980), is an interesting alternative to the commonly applied numerical methods of solving the partial differential equations. The calculations are run on the basis of the enforcement of flux conservation (which is also the basic assumption of the Finite Volume Method), but the distinguishing feature of the STC method is the unification of space and time, and treating them on the same footing. Such approach leads to the construction of the "space-time" cells (in 1D problem – the rectangles in the x-t plane), in which the flux conservation is enforced.

The STC scheme, applied to solve the classical initial-boundary problem for Saint-Venant equations (Molls and Molls 1998), is the modification of the scheme called „$a - \mu$" (Chang 1995), which was originally applied to solve the advection-diffusion equation. As it occurs (Weinerowska 2001), the STC scheme may also be successfully used to solve the reverse flow routing problem. It requires some necessary modifications and finally leads to the algorithm the numerical properties of which are better than in the case of the methods used so far e.g. the four-point scheme. The short description of the STC scheme applied to the direct problem of flow routing was presented by Molls and Molls (1998), also, the detailed analyses, including the questions of stability and accuracy, were developed by Weinerowska (2001). In the next section the application of the STC scheme to the inverse problem for Saint-Venant equations is presented.

2. Solution to the RFR Problem by the STC Method

Let the system of the Saint–Venant equations be written in its conservation form as

$$\frac{\partial \mathbf{f}}{\partial t} + \frac{\partial \mathbf{G}}{\partial x} = \mathbf{S}, \tag{3a}$$

where

$$\mathbf{f} = \begin{Bmatrix} A \\ Q \end{Bmatrix}, \quad \mathbf{G} = \begin{Bmatrix} Q \\ \frac{Q^2}{A} + g I_1 \end{Bmatrix}, \quad \mathbf{S} = \begin{Bmatrix} 0 \\ gA(S_o - S_f) \end{Bmatrix}. \tag{3b}$$

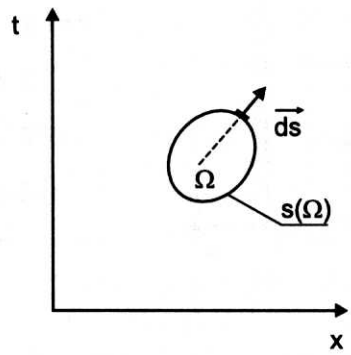

Fig. 2. Area Ω in the x-t plane

The solution in 2D space-time (x, t) – in which the element of an area Ω and the boundary $s(\Omega)$ (Fig. 2) is established – is searched. For the chosen element the flux conservation is enforced and the Eq. (3a) is demanded to be satisfied. The vectorial Eq. (3a) is the differential form of the conservation laws, the integral form of which may be achieved by applying Green's theorem (Peyret and Taylor 1983):

$$\iint_{\Omega} \left(\frac{\partial \mathbf{f}}{\partial t} + \frac{\partial \mathbf{G}}{\partial x} \right) d\Omega = \oint_{s(\Omega)} \mathbf{f} dx - \mathbf{G} dt = \oint_{s(\Omega)} \mathbf{h} ds,$$

where $\mathbf{h} = (\mathbf{G}, \mathbf{f})$, and $\mathbf{h}ds$ represents the space-time flux of $\mathbf{h}$ through $s(\Omega)$. The integration along the boundary of the Ω domain is run anti-clockwise (Dziubiński and Świątkowski 1985).

The integral form of Eq. (3a) is

$$\oint_{s(\Omega)} \mathbf{h} ds = \oint_{s(\Omega)} \mathbf{f} dx - \mathbf{G} dt = \iint_{\Omega} \mathbf{S} d\Omega. \tag{4}$$

It can be seen that the unification of x and t variables is applied. They are treated in the same manner, and the integrating is run along the $s(\Omega)$ curve in the $(x,$

t) plane. Such approach is considerably different from those of other methods, including Final Volume Method, applied for the volumes in geometrical space (Szydłowski 1998).

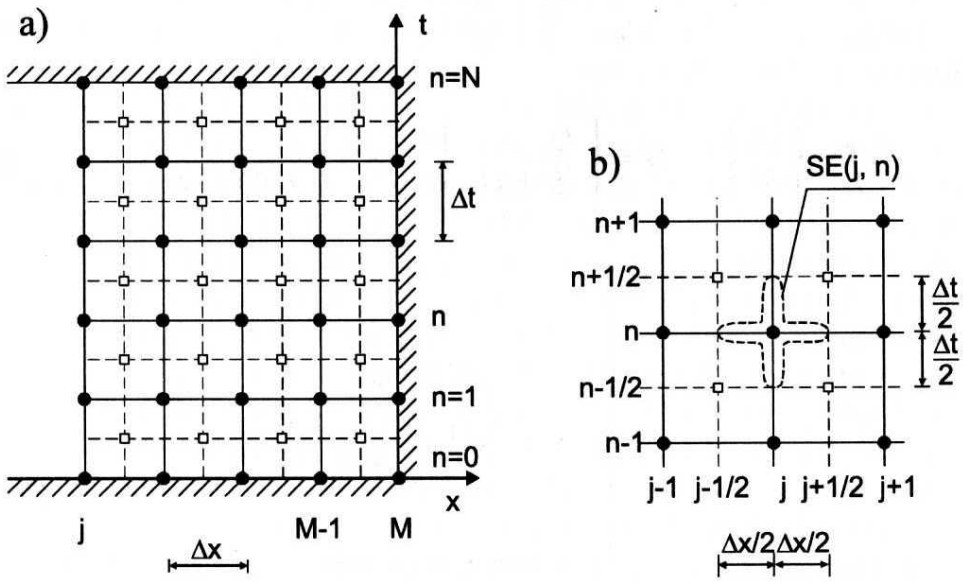

Fig. 3. a) Computational grid in the inverse problem solved by the STC scheme, b) solution element (j,n)

The solution domain in an inverse problem is covered with the set of nodal points (j, n), described by indices $j = M, M-1, \ldots$ and $n = 0, 1, \ldots, N$ (Fig. 3a). The grid constructed in such a way is additionally covered by a set of intermediate points in the middle of each mesh, with the indices $(j \pm 1/2,\ n \pm 1/2)$ for $j = M-1,\ M-2, \ldots; n = 1, 2, 3, \ldots N-1$. In consequence, a grid as in Fig. 3a is obtained. While the values in the nodes at the $j+1$ cross section are known, the calculation of the unknown values at the j cross section is run in two stages. First the values in the intermediate points at the $j+1/2$ cross section are computed, then – according to the same formulas – the next step from $j+1/2$ to j is made.

Every mesh point of the grid is associated with a solution element SE, that consists of vertical and horizontal segments of the grid (lengths of which are $\Delta t/2$ and $\Delta x/2$, respectively), protruding from the referred mesh point in the positive and negative direction of t and x axes, and the closest neighbourhood of these segments. For example, the SE connected with the node (j, n), defined as an interior of the space-time region bounded by a dashed curve, is shown in Fig. 3b.

For any $(x, t) \in \mathrm{SE}(j, n)$ variables **f** and **G** are approximated by **f*** i **G*** according to formulae:

$$\mathbf{f}^*(x, t; j, n) = \mathbf{f}_j^n + (\mathbf{f}_x)_j^n (x - x_j) + (\mathbf{f}_t)_j^n (t - t^n), \tag{5a}$$

$$\mathbf{G}^*(x,t;j,n) = \mathbf{G}_j^n + (\mathbf{G}_x)_j^n(x - x_j) + (\mathbf{G}_t)_j^n(t - t^n), \tag{5b}$$

where: $\mathbf{f}_j^n$, $(\mathbf{f}_x)_j^n$, $(\mathbf{f}_t)_j^n$ and $\mathbf{G}_j^n$, $(\mathbf{G}_x)_j^n$, $(\mathbf{G}_t)_j^n$ respectively are constant in SE(j, n) and (x_j, t^n) are the coordinates of the node (j, n). As results from Eq. (5a) and (5b):

$$\mathbf{f}^*(x_j, t^n; j, n) = \mathbf{f}_j^n, \tag{6a}$$

$$\frac{\partial \mathbf{f}^*}{\partial x}(x_j, t^n; j, n) = (\mathbf{f}_x)_j^n, \quad \frac{\partial \mathbf{f}^*}{\partial t}(x_j, t^n; j, n) = (\mathbf{f}_t)_j^n, \tag{6b, c}$$

and for **G** respectively.

The values of the variables $\mathbf{f}_j^n$, $(\mathbf{f}_x)_j^n$ and $(\mathbf{f}_t)_j^n$, which occur in formula (5a), may be identified as the values of the function **f** and its $\partial\mathbf{f}/\partial x$ and $\partial\mathbf{f}/\partial t$ in the node (j, n) (for **G** analogously (5b)). As the result, the right side expressions in (5a) and (5b) become first order Taylor series expansions of **f** and **G** around the node (j, n). Thus, the values of $\mathbf{f}_j^n$, $(\mathbf{f}_x)_j^n$ i $(\mathbf{f}_t)_j^n$ may be treated as the numerical equivalents of **f** and its derivatives $\partial\mathbf{f}/\partial x$ and $\partial\mathbf{f}/\partial t$ (for **G** respectively) in the node (j, n). Moreover, $\mathbf{f} = \mathbf{f}^*(x, t; j, n)$ and $\mathbf{G} = \mathbf{G}^*(x, t; j, n)$ should satisfy the Eq. (3a), which implies that

$$(\mathbf{G}_x)_j^n = \mathbf{S}_j^n - (\mathbf{f}_t)_j^n. \tag{7}$$

It is required that Eq. (4), which is the integral form of Eq. (3a), is satisfied in the whole domain, which means the global flux conservation. In addition, also the local flux conservation is required. This local flux conservation refers to the particular cells, called the „Conservation Elements" (CE). These CE are the rectangles on the (x, t) plane, with the length of the sides $\Delta x/2$ and $\Delta t/2$. Each CE is defined by two nodes on the diagonal of the rectangle and each solution element SE is associated with four CEs (Fig. 4a).

Any segment that is a side of the CE (e.g. AB in Fig. 4b) is also an interface separating two adjoin cells (e.g. $\mathrm{CE}^-(j,n)$ i $\mathrm{CE}^+(j,n)$). The flux through this interface is evaluated using the information from only one SE (SE(j, n)).

In each cell CE flux conservation is required. The values of **f** and **G** for each cell are approximated by $\mathbf{f}^*$ and $\mathbf{G}^*$ according to formulas (5a) and (5b) for suitable solution elements SE that constitute the cell boundary. As the boundary of each cell is constructed by segments belonging to two neighbouring solution elements SE, only the values from two nodes appear in the conservation equation for each cell. One node is from the "known" cross section and one is from the "unknown" one.

Let the $j + 1/2$ cross section variables be known and variables in j cross section searched. The values of any function computed in the node (j, n) depend on the information from $\mathrm{CE}^-(j,n)$ and $\mathrm{CE}^+(j,n)$ only (Fig. 4b).

Let

$$F^+(j,n) = \oint_{s\left(CE^+_{(j,n)}\right)} -\mathbf{G}^*dt + \mathbf{f}^*dx = F^+, \tag{8a}$$

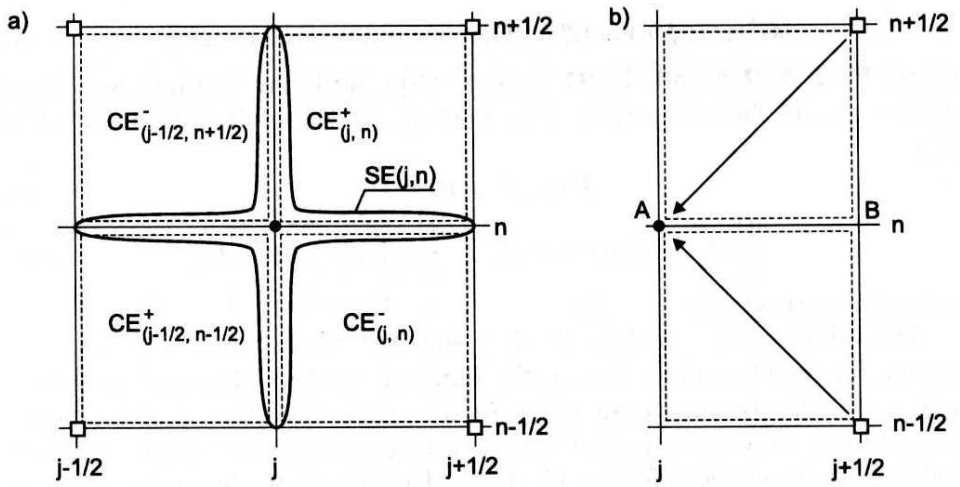

Fig. 4. a) Structure of the cells associated with solution element SE (j, n), b) cells taking part in evaluation of functions and their derivatives (j, n)

$$F^-(j,n) = \oint\limits_{s\left(CE^-_{(j,n)}\right)} -\mathbf{G}^* dt + \mathbf{f}^* dx = F^-. \tag{8b}$$

Substituting (5a), (5b) in Eq. (8a), (8b) and integrating along the boundary of $\mathrm{CE}^+(j,n)$ and $\mathrm{CE}^-(j,n)$ yields

$$\frac{2}{\Delta x}F^+ = -\mathbf{f}_j^n - \frac{\Delta x}{4}(\mathbf{f}_x)_j^n - \frac{\Delta t}{\Delta x}\mathbf{G}_j^n - \frac{(\Delta t)^2}{4\Delta x}(\mathbf{G}_t)_j^n + \mathbf{f}_{j+1/2}^{n+1/2} - \mathbf{W}_{j+1/2}^{n+1/2}, \tag{9a}$$

$$\frac{2}{\Delta x}F^- = \mathbf{f}_j^n + \frac{\Delta x}{4}(\mathbf{f}_x)_j^n - \frac{\Delta t}{\Delta x}\mathbf{G}_j^n + \frac{(\Delta t)^2}{4\Delta x}(\mathbf{G}_t)_j^n - \mathbf{f}_{j+1/2}^{n-1/2} + \mathbf{W}_{j+1/2}^{n-1/2}, \tag{9b}$$

where

$$\mathbf{W}_{j+1/2}^{n\pm1/2} = \frac{\Delta x}{4}(\mathbf{f}_x)_{j+1/2}^{n\pm1/2} \mp \frac{\Delta t}{\Delta x}\mathbf{G}_{j+1/2}^{n\pm1/2} + (\mathbf{G}_t)_{j+1/2}^{n\pm1/2}\frac{(\Delta t)^2}{4\Delta x}. \tag{9c}$$

According to (4) it is required that

$$F^+ = \iint\limits_{\Omega(CE^+)} \mathbf{S}^* d\Omega = S^+, \tag{10a}$$

$$F^- = \iint\limits_{\Omega(CE^-)} \mathbf{S}^* d\Omega = S^-, \tag{10b}$$

and in the case of lack of the source terms

$$F^+ = 0, \tag{11a}$$

$$F^- = 0. \tag{11b}$$

The vector $\mathbf{S}^*$ in Eq. (10a, b) is determined as follows:

- in CE$^-$:

$$\mathbf{S}^* = \mathbf{S}_{j+1/2}^{n-1/2} + (\mathbf{S}_x)_{j+1/2}^{n-1/2}\left(x - x_{j+1/2}\right) + (\mathbf{S}_t)_{j+1/2}^{n-1/2}\left(t - t^{n-1/2}\right), \tag{12a}$$

- in CE$^+$:

$$\mathbf{S}^* = \mathbf{S}_{j+1/2}^{n+1/2} + (\mathbf{S}_x)_{j+1/2}^{n+1/2}\left(x - x_{j+1/2}\right) + (\mathbf{S}_t)_{j+1/2}^{n+1/2}\left(t - t^{n+1/2}\right), \tag{12b}$$

thus

$$S^+ = \mathbf{S}_{j+1/2}^{n+1/2}\frac{\Delta x\,\Delta t}{4} - (\mathbf{S}_x)_{j+1/2}^{n+1/2}\frac{\Delta t\,(\Delta x)^2}{16} - (\mathbf{S}_t)_{j+1/2}^{n+1/2}\frac{\Delta x\,(\Delta t)^2}{16}, \tag{13a}$$

$$S^- = \mathbf{S}_{j+1/2}^{n-1/2}\frac{\Delta x\,\Delta t}{4} - (\mathbf{S}_x)_{j+1/2}^{n-1/2}\frac{\Delta t\,(\Delta x)^2}{16} + (\mathbf{S}_t)_{j+1/2}^{n-1/2}\frac{\Delta x\,(\Delta t)^2}{16}, \tag{13b}$$

where

$$\mathbf{S}_x = \frac{\partial \mathbf{S}}{\partial \mathbf{f}}\mathbf{f}_x = \frac{\partial \mathbf{S}}{\partial \mathbf{f}}\left(\frac{\partial \mathbf{G}}{\partial \mathbf{f}}\right)^{-1}(\mathbf{S} - \mathbf{f}_t), \tag{14a}$$

$$\mathbf{S}_t = \frac{\partial \mathbf{S}}{\partial \mathbf{f}}\mathbf{f}_t. \tag{14b}$$

Substituting the formulas for F^+ and F^- (9a, b) and for S^+ and S^- (13a, b) in Eq. (10 a, b) or (11a, b) yields the set of two vectorial equations with two vectorial unknowns treated independently – $\mathbf{f}_j^n$ and $(\mathbf{f}_t)_j^n$, as all the other variables computed in the unknown cross section j, may be expressed as the combination of the two above:

$$\mathbf{f}_x = \left(\frac{\partial \mathbf{G}}{\partial \mathbf{f}}\right)^{-1}(\mathbf{S} - \mathbf{f}_t), \tag{15a}$$

$$\mathbf{G}_t = \left(\frac{\partial \mathbf{G}}{\partial \mathbf{f}}\right)\mathbf{f}_t. \tag{15b}$$

However, it is not possible to obtain the explicit formulaş for $\mathbf{f}$ and $\mathbf{f}_t$, as the system of the non-linear equations of a relatively complex form is achieved. Much simpler formulas are obtained if the values of $\mathbf{G}$ and $\mathbf{G}_t$ are determined from this system and then the values of $\mathbf{f}$ and $\mathbf{f}_t$ are computed.

Unfortunately, if this approach is applied in the form presented above, the calculations do not lead to a successful result, as the solution suffers from considerable numerical errors. The same problem may be observed in the case of direct problems. Thus the scheme presented requires some modifications.

Applying such an approach to the direct problem for the advection-diffusion equation Chang (1995) showed that in the case of pure advection the absolute

value of the amplification factor for this scheme is equal to unity irrespective of the grid size. This means that the scheme is always non-dissipative. The accuracy analysis shows in addition, that the scheme is dispersive, and only for the Courant number equal to unity does the dispersion disappear. As in real cases it is not possible to run the computations with $C_r = 1$, in consequence, a solution suffering from unphysical oscillations is obtained. In order to improve the properties of the scheme, Chang (1995) presented its modification by introducing on the right sides of the equations (11a, b) non-zero terms, responsible for numerical dissipation. The magnitude of such terms depends on the values of the derivatives on the known time level and from a numerical parameter ($0 \leq \varepsilon \leq 1$), irrespective of any other variables. The numerical dissipation is controlled by the value of the parameter ε which can be modified in the scheme. For $\varepsilon = 0$ the values of the additional terms are equal to zero (no numerical dissipation). The terms introduced into the equations are of the same magnitude, but opposite signs (positive for F^+, negative for F^-). As a result, in each of the cells CE^+ and CE^- the conservation law is not satisfied and the symmetry is broken. However, the conservation law is satisfied in CE, which is the sum of CE^+ and CE^-, as the artificially introduced terms are reduced.

The modified approach proposed by Chang (1995) for the advection-diffussion equation may also be successfully applied in the case of the inverse problem. The conservation law for CE, which is the sum of CE^+ and CE^-, may be written as follows:

$$F^+ + F^- = \oint_{s(CE^+(j,n))} -\mathbf{G}^* dt + \mathbf{f}^* dx + \oint_{s(CE^-(j,n))} -\mathbf{G}^* dt + \mathbf{f}^* dx = \int\int_{\Omega(CE^+)} \mathbf{S}^* d\Omega + \int\int_{\Omega(CE^-)} \mathbf{S}^* d\Omega = S^+ + S^-, \tag{16a}$$

that is

$$\frac{2}{\Delta x}\left(F^+ + F^-\right) = \frac{2}{\Delta x}\left(S^+ + S^-\right), \tag{16b}$$

where F^+ and F^- are obtained from Eq. (9a, b, c) and S^+ and S^- from (13a, b).

The formulas for $\mathbf{G}$ and $\mathbf{G}_t$ obtained by solving the modified system of equations are as follows:

$$\mathbf{G}_j^n = \frac{1}{2}\left\{\frac{\Delta x}{\Delta t}\cdot\left(\mathbf{f}_{j+1/2}^{n+1/2} - \mathbf{f}_{j+1/2}^{n-1/2} + \mathbf{W}_{j+1/2}^{n-1/2} - \mathbf{W}_{j+1/2}^{n+1/2}\right) - \mathbf{E}\right\}, \tag{17a}$$

where:

$$\mathbf{E} = \frac{\Delta x}{8}\left\{4\left(\mathbf{S}_{j+1/2}^{n-1/2} + \mathbf{S}_{j+1/2}^{n+1/2}\right) - \Delta x\left[(\mathbf{S}_x)_{j+1/2}^{n-1/2} + (\mathbf{S}_x)_{j+1/2}^{n+1/2}\right] + \Delta t\left[(\mathbf{S}_t)_{j+1/2}^{n-1/2} - (\mathbf{S}_t)_{j+1/2}^{n+1/2}\right]\right\}, \tag{17b}$$

and

$$(\mathbf{G}_t)_j^n = \frac{\mathbf{G}_j^{n+1/2} - \mathbf{G}_j^{n-1/2}}{\Delta t} + (2\varepsilon - 1) \cdot (d\mathbf{G}_t)_j^n , \tag{18}$$

where:

$$(d\mathbf{G}_t)_j^n = \frac{(\mathbf{G}_t)_{j+1/2}^{n+1/2} + (\mathbf{G}_t)_{j+1/2}^{n-1/2}}{2} - \frac{\mathbf{G}_{j+1/2}^{n+1/2} - \mathbf{G}_{j+1/2}^{n-1/2}}{\Delta t}, \tag{19}$$

$$\mathbf{G}_j^{n\pm1/2} = \mathbf{G}_{j+1/2}^{n\pm1/2} - \frac{\Delta x}{2} \cdot (\mathbf{G}_x)_{j+1/2}^{n\pm1/2}, \tag{20}$$

and $\mathbf{G}_x$ in any node is obtained according to Eq. (7).

According to the definition

$$\mathbf{G} = \begin{Bmatrix} Q \\ \frac{Q^2}{A} + g I_1, \end{Bmatrix} \tag{21}$$

the values of Q and Q_t may be determined explicitly; the remaining unknowns are the result of solving the non-linear equations:

$$\frac{Q^2}{A} + g I_1 = G_2, \quad \frac{\partial \left(\frac{Q^2}{A} + g I_1 \right)}{\partial t} = (G_t)_2 , \tag{22a, b}$$

where G_2 and $(G_t)_2$ are the second co-ordinates of the column vectors $\mathbf{G}$ and $\mathbf{G}_t$.

Thus the computing of the values in cross-section j on the basis of known values in the cross-section $j+1$ is run in two stages. Each stage requires computations that can be characterised by three steps. For example, when computing the values of the j cross-section when the values of the $j+1/2$ cross-section are known, the following three steps are carried out:

step Ia: calculations of $\mathbf{G}$ in the nodes $(j, n \pm k)$ for $k = 0, 1, 2, \ldots$ according to formulas (17a, b);

step Ib: calculation of $\mathbf{f}$ in the nodes $(j, n \pm k)$ for $k = 0, 1, 2, \ldots$;

step II: calculation of $\mathbf{G}$ in the nodes $(j, n \pm m \cdot \frac{1}{2})$ for $m = 1, 3, 5, \ldots$ according to formula (20);

step IIIa: calculation of derivatives $\mathbf{G}_t$ in the nodes $(j, n \pm k)$ for $k = 0, 1, 2, \ldots$ according to formula (18);

step IIIb: calculation of derivatives $\mathbf{f}_t$ in the nodes $(j, n \pm k)$ for $k = 0, 1, 2$.

The sequence of the computations and flow of information on the computational grid are shown in Fig. 5.

3. Stability Analysis

More information concerning features of the numerical scheme may be achieved by investigating its stability. It is usually examined for the following linear system

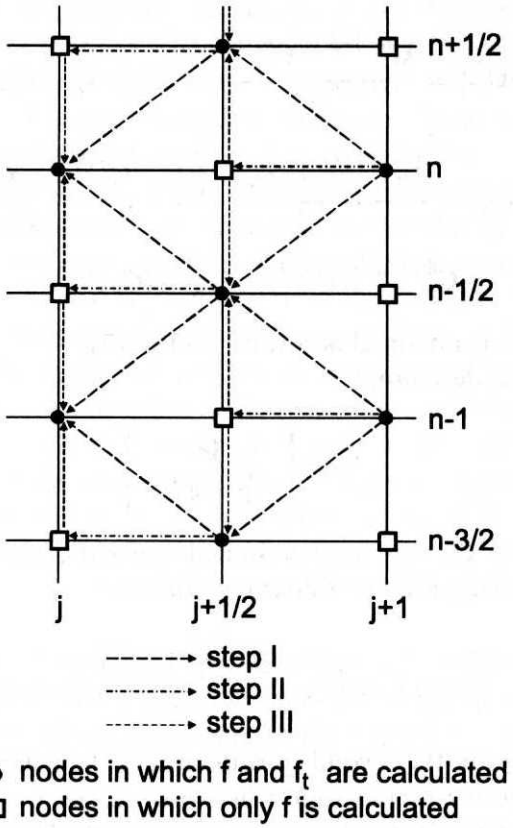

Fig. 5. Scheme of the flow of information on the computational grid in reverse flow routing problem solved by STC method

of partial differential equations (Szymkiewicz 1996):

$$\frac{\partial H}{\partial t} + \overline{H}\frac{\partial U}{\partial x} = 0, \tag{23a}$$

$$\frac{\partial U}{\partial t} + g\frac{\partial H}{\partial x} = 0, \tag{23b}$$

where $\overline{H}$ is the constant average flow depth. The system (23a, b) can be obtained by the simplification of the Saint-Venant system of equations and vectors **f** and **G** in this case are as follows:

$$\mathbf{f} = \begin{Bmatrix} H \\ U \end{Bmatrix}, \quad \mathbf{G} = \begin{Bmatrix} \overline{H}U \\ gH \end{Bmatrix}. \tag{24a, b}$$

Applying the formulas (17 ÷ 20) to solve (23a, b), the system of equations that may be written in the following form is obtained:

$$\mathbf{t}(j,n) = \mathbf{P}_+ \mathbf{t}\left(j+\frac{1}{2}, n-\frac{1}{2}\right) + \mathbf{P}_- \mathbf{t}\left(j+\frac{1}{2}, n+\frac{1}{2}\right), \tag{25}$$

where

$$\mathbf{t}(i,m) = \begin{pmatrix} U_i^m \\ \frac{\Delta t}{4}(U_t)_i^m \\ H_i^m \\ \frac{\Delta t}{4}(H_t)_i^m \end{pmatrix}. \tag{26}$$

$$\mathbf{P}_+ = \frac{1}{2}\begin{bmatrix} 1 & 1-K^2 & -\frac{\Delta x}{\Delta t\,\overline{H}} & 0 \\ \varepsilon - 1 & 2\varepsilon - 1 & 0 & -\frac{\Delta x}{\Delta t\,\overline{H}} \\ -\frac{\Delta x}{\Delta t\, g} & 0 & 1 & 1-K^2 \\ 0 & -\frac{\Delta x}{\Delta t\, g} & \varepsilon - 1 & 2\varepsilon - 1 \end{bmatrix},$$

$$\mathbf{P}_- = \frac{1}{2}\begin{bmatrix} 1 & -(1-K^2) & \frac{\Delta x}{\Delta t\,\overline{H}} & 0 \\ 1-\varepsilon & 2\varepsilon - 1 & 0 & \frac{\Delta x}{\Delta t\,\overline{H}} \\ \frac{\Delta x}{\Delta t\, g} & 0 & 1 & -(1-K^2) \\ 0 & \frac{\Delta x}{\Delta t\, g} & 1-\varepsilon & 2\varepsilon - 1 \end{bmatrix} \tag{27}$$

and

$$K = \frac{1}{C_r} = \frac{\Delta x}{\sqrt{g\overline{H}}\,\Delta t} \tag{28}$$

is the inverse of the Courant number.

As

$$\mathbf{t}\left(j+\frac{1}{2}, n-\frac{1}{2}\right) = \mathbf{P}_+\,\mathbf{t}(j+1, n-1) + \mathbf{P}_-\,\mathbf{t}(j+1, n), \tag{29a}$$

$$\mathbf{t}\left(j+\frac{1}{2}, n+\frac{1}{2}\right) = \mathbf{P}_+\,\mathbf{t}(j+1, n) + \mathbf{P}_-\,\mathbf{t}(j+1, n+1), \tag{29b}$$

the full transition from the cross-section $j+1$ to cross-section j is carried out in accordance with the formula

$$\begin{aligned}\mathbf{t}(j,n) = (\mathbf{P}_+)^2\mathbf{t}(j+1, n-1) + (\mathbf{P}_+\mathbf{P}_- + \mathbf{P}_-\mathbf{P}_+)\,\mathbf{t}(j+1, n) + \\ +(\mathbf{P}_-)^2\mathbf{t}(j+1, n+1)\end{aligned}, \tag{30}$$

where: $(\mathbf{P}_+)^2 = \mathbf{P}_+\mathbf{P}_+$, $(\mathbf{P}_-)^2 = \mathbf{P}_-\mathbf{P}_-$.

Applying the von Neumann stability analysis (Fletcher 1991), functions U, H and U_t, H_t that appear in (26) and (27), are extended into the finite Fourier series and the behaviour of the single k component when passing from $j+1$ to j is examined. It can be proved (Weinerowska 2001), that the amplification matrix $\mathbf{A}$ in this case may be written as

$$\begin{aligned}\mathbf{A} &= \mathbf{P}_+\mathbf{P}_+ \cdot e^{-ik\Delta t} + (\mathbf{P}_+\mathbf{P}_- + \mathbf{P}_-\mathbf{P}_+) + \mathbf{P}_-\mathbf{P}_- e^{ik\Delta t} = \\ &= \left[\mathbf{P}_+ e^{-ik\frac{\Delta t}{2}} + \mathbf{P}_- e^{ik\frac{\Delta t}{2}}\right]^2 = \mathbf{P}^2,\end{aligned} \tag{31}$$

where

$$\mathbf{P} = \begin{bmatrix} p_{11} & p_{12} & p_{13} & p_{14} \\ p_{21} & p_{22} & p_{23} & p_{24} \\ p_{31} & p_{32} & p_{33} & p_{34} \\ p_{41} & p_{42} & p_{43} & p_{44} \end{bmatrix}, \tag{32}$$

$$p_{11} = p_{33} = \cos\left(\frac{\varphi}{2}\right), \qquad p_{12} = p_{34} = (K^2 - 1)i \sin\left(\frac{\varphi}{2}\right),$$

$$p_{13} = p_{24} = \frac{\Delta x}{\Delta t \overline{H}} i \sin\left(\frac{\varphi}{2}\right), \qquad p_{31} = p_{42} = \frac{x \Delta x}{\Delta t\, g} i \sin\left(\frac{\varphi}{2}\right),$$

$$p_{21} = p_{43} = (1 - \varepsilon)i \sin\left(\frac{\varphi}{2}\right), \qquad p_{22} = p_{44} = (2\varepsilon - 1) \cos\left(\frac{\varphi}{2}\right),$$

$$p_{14} = p_{23} = p_{32} = p_{41} = 0$$

and $\varphi = k\Delta t$.

It is known (Fletcher 1991), that any scheme is numerically stable if the greatest modulus of eigenvalue of the amplification matrix is not greater than unity, i.e.

$$|\lambda| \leq 1. \tag{33}$$

The eigenvalues of **P** obtained from the condition

$$\det[\mathbf{P} - \lambda \mathbf{I}] = 0 \tag{34}$$

are

$$\lambda_{++} = \varepsilon \cdot \cos\left(\frac{\varphi}{2}\right) + Ki \sin\left(\frac{\varphi}{2}\right) + R, \tag{35a}$$

$$\lambda_{+-} = \varepsilon \cdot \cos\left(\frac{\varphi}{2}\right) + Ki \sin\left(\frac{\varphi}{2}\right) - R, \tag{35b}$$

$$\lambda_{-+} = \varepsilon \cdot \cos\left(\frac{\varphi}{2}\right) - Ki \sin\left(\frac{\varphi}{2}\right) + R, \tag{35c}$$

$$\lambda_{--} = \varepsilon \cdot \cos\left(\frac{\varphi}{2}\right) - Ki \sin\left(\frac{\varphi}{2}\right) - R, \tag{35d}$$

where

$$R = \sqrt{(1 - \varepsilon)\left[(1 - \varepsilon) \cos^2\left(\frac{\varphi}{2}\right) + (1 - K^2) \sin^2\left(\frac{\varphi}{2}\right)\right]}, \tag{36}$$

and $\varepsilon \in < 0, 1 >$ and $K \leq 1$.

The eigenvalues of **A** satisfy the conditions

$$\lambda_{A^{++}} = (\lambda_{++})^2, \quad \lambda_{A^{--}} = (\lambda_{--})^2, \quad \lambda_{A^{+-}} = (\lambda_{+-})^2, \quad \lambda_{A^{-+}} = (\lambda_{-+})^2. \tag{37}$$

The modulus of the eigenvalues of **P** is

$$|\lambda| = \left\{\left[\varepsilon \cos\left(\frac{\varphi}{2}\right) \pm R\right] + K^2 \sin^2\left(\frac{\varphi}{2}\right)\right\}^{1/2}, \tag{38a}$$

and for **A**

$$|\lambda_A| = (|\lambda|)^2 = \left[\varepsilon \cos\left(\frac{\varphi}{2}\right) \pm R\right]^2 + K^2 \sin^2\left(\frac{\varphi}{2}\right). \tag{38b}$$

Analysis of (38b) in the light of (33) leads to the following conclusions:

- for $\varepsilon \in < 0, 1 >$ and $K \leq 1$ ($C_r \geq 1$) the values of $|\lambda|$ are in the range of $< 0, 1 >$, thus the scheme is stable then;
- for $\varepsilon = 0$ and $K \leq 1$ we obtain

$$\lambda_A = 1 - 2K^2 \sin^2\left(\frac{\varphi}{2}\right) \pm 2Ki \sin\left(\frac{\varphi}{2}\right) \sqrt{1 - K^2 \sin^2\left(\frac{\varphi}{2}\right)} \tag{39a}$$

and

$$|\lambda_A| = 1, \tag{39b}$$

which means that the wave amplitude is neither damped nor amplified and the scheme does not produce the numerical diffusion;

- for $\varepsilon \neq 0$ and $K < 1$ ($C_r > 1$) the scheme generates numerical dissipation, the magnitude of which depends on the value of ε;
- for $\varepsilon \neq 0$ and $K = 1$ the scheme is non-dissipative as

$$|\lambda_{A_{++}}| = |\lambda_{A_{+-}}| = 1.$$

Detailed information about numerical errors introduced by a scheme may be achieved from the accuracy analysis.

4. Accuracy Analysis

After replacing the node values in (30) by their Taylor series extensions around the node $(j + 1, n)$ and after putting the expressions obtained in order, the following equations are obtained:

$$\frac{\partial H}{\partial t} + \overline{H}\frac{\partial U}{\partial x} = -\frac{(\Delta t)^2}{24}(1 - K^2)\frac{\partial^3 H}{\partial t^3} + \frac{\overline{H}(\Delta t)^4}{48\Delta x}\varepsilon(1 - K^2)\frac{\partial^4 U}{\partial t^4} + \\ -\frac{\overline{H}(\Delta t)^4}{24\Delta x}K^2(1 - K^2)\frac{\partial^4 U}{\partial t^4}, \tag{40a}$$

$$\frac{(\Delta t)^3}{48}(4\varepsilon^2 - \varepsilon - 3\varepsilon K^2)\frac{\partial^3 U}{\partial t^3} + \frac{(\Delta x)(\Delta t)^3}{24\overline{H}}\left(\varepsilon - K^2\right)\frac{\partial^4 H}{\partial t^4} = 0, \tag{40b}$$

$$\frac{\partial U}{\partial t} + g\frac{\partial H}{\partial x} = -\frac{(\Delta t)^2}{24}(1 - K^2)\frac{\partial^3 U}{\partial t^3} + \frac{g(\Delta t)^4}{48\Delta x}\varepsilon(1 - K^2)\frac{\partial^4 H}{\partial t^4} + \\ -\frac{g(\Delta t)^4}{24\Delta x}K^2(1 - K^2)\frac{\partial^4 H}{\partial t^4}, \tag{40c}$$

$$\frac{(\Delta t)^3}{48}(4\varepsilon^2 - \varepsilon - 3\varepsilon K^2)\frac{\partial^3 H}{\partial t^3} + \frac{(\Delta x)(\Delta t)^3}{24g}\left(\varepsilon - K^2\right)\frac{\partial^4 U}{\partial t^4} = 0. \tag{40d}$$

The equations (40a, c) may be written (using the information from (40b, d)) as

$$\frac{\partial H}{\partial t} + \overline{H}\frac{\partial U}{\partial x} = \varepsilon_{11}\frac{\partial^3 U}{\partial t^3} + \varepsilon_{12}\frac{\partial^3 H}{\partial t^3} + \gamma_{11}\frac{\partial^4 U}{\partial t^4} + \gamma_{12}\frac{\partial^4 H}{\partial t^4}. \tag{41a}$$

$$\frac{\partial U}{\partial t} + g\frac{\partial H}{\partial x} = \varepsilon_{21}\frac{\partial^3 U}{\partial t^3} + \varepsilon_{22}\frac{\partial^3 H}{\partial t^3} + \gamma_{21}\frac{\partial^4 U}{\partial t^4} + \gamma_{22}\frac{\partial^4 H}{\partial t^4}. \tag{41b}$$

where:

$$\varepsilon_{11} = \varepsilon_{22} = 0, \tag{41c}$$

$$\varepsilon_{12} = \varepsilon_{21} = -\frac{(\Delta t)^2(1 - K^2)}{48K^2}\left[\varepsilon(4\varepsilon - 3K^2 - 1) + 2K^2\right] \tag{41d}$$

and

$$\gamma_{11} = -\frac{\overline{H}(\Delta t)^4}{48(\Delta x)}\varepsilon(1 - K^2), \qquad \gamma_{22} = -\frac{g(\Delta t)^4}{48(\Delta x)}\varepsilon(1 - K^2), \tag{41e, f}$$

$$\gamma_{12} = \gamma_{21} = 0. \tag{41g}$$

Analysis of (40) and (41) leads to the conclusions:

- the scheme leads to algebraic equations that are coincident with the differential ones. For Δx, $\Delta t \to 0$ the right hand terms of (40a, c) and all terms of (40b, d) tend to zero, thus the modified equations tend to the governing system (23a, b);
- in the general case, the modified equations (41a,b) include third-order derivative terms and higher; this means that the scheme is of second order accuracy, it generates numerical dispersion connected with the third order derivative and numerical dissipation resulting from the fourth order terms;
- for $K = 1$ the coefficients ε_{12}, ε_{21} and γ_{11}, γ_{22} are of zero value irrespective of the value of ε. This means that for $K = 1$ the accurate solution is obtained;
- for $\varepsilon = 0$ the modified equations are simplified to:

$$\frac{\partial H}{\partial t} + \overline{H}\frac{\partial U}{\partial x} = -\frac{(\Delta t)^2(1 - K^2)}{24}\frac{\partial^3 H}{\partial t^3}, \tag{42a}$$

$$\frac{\partial U}{\partial t} + g\frac{\partial H}{\partial x} = -\frac{(\Delta t)^2(1 - K^2)}{24}\frac{\partial^3 U}{\partial t^3}. \tag{42b}$$

The even order derivatives disappear from the right sides of these equations which results in the lack of numerical dissipation in this case. Such conclusion is coincident with the results of the stability analysis for $\varepsilon = 0$ and $K < 1$, when the scheme is non-dissipative but dispersive. Numerical dispersion vanishes when $K = 1$, which gives the accurate solution;

- if K is constant, the coefficients ε_{12} and ε_{21} are of the least value when

$$\varepsilon = \frac{1+3K^2}{8}. \tag{43}$$

For the maximum possible value of K which is equal to unity, the value of this coefficient is $\varepsilon = 0.5$. With increasing value of ε the absolute values of γ_{11} and γ_{22} responsible for numerical dissipation, also increase.

The values of the coefficients given above were obtained as the result of the analysis of the linear problem. For non-linear problems the optimal value of ε is difficult to determine. It is also difficult to estimate the magnitude of numerical dissipation and dispersion. However, according to the analysis presented, it seems reasonable to assume $\varepsilon = 0.5$ or to determine this parameter on the ground of the analysis of the specific practical cases.

5. Numerical Tests

The successful testing of the properties of the scheme and appraising the quality of the numerical results, can be obtained by solving the inverse problem after previously solving the direct problem, as the required and obtained results may be compared. The tests presented below concern the solution of the Saint-Venant equations in a rectangular channel with constant bottom slope. In both cases the postulated discharge functions in upstream cross-section were imposed, the direct problem was solved and the referred functions of $Q_L(t)$ and $h_L(t)$ in the downstream cross-section obtained. These functions were next imposed as the downstream conditions, the inverse problems were solved and the obtained and required discharge functions $Q_0(t)$ compared. In both cases the flow resistance was expressed by the Manning formula. The direct problem in both cases was solved twice: by applying the implicit four-point scheme and STC scheme. Comparison of the solutions proved that in the case of direct problems, both schemes lead to successful solution of comparable accuracy. In further analysis, the solution achieved by the STC scheme was applied, as this provided better mass conservation.

Test 1

The rectangular channel of the constant bottom slope $S_o = 0.0001$, length $L = 50$ km, width 50 m, and constant Manning coefficient $n = 0.02$ is considered. The channel is divided into 50 distance intervals of length $\Delta x = 1000$ m, which gives $M = 51$ cross-sections. At time $t = 0$ the condition of steady uniform flow is imposed. The water depth is $H = 2.5$ m, and the discharge $Q = 108.038$ m^3/s. The imposed discharge function in upstream cross-section $Q_0(t)$ is shown in Fig. 6a. It is also the upstream condition in the direct problem. Such a severe kind of condition was chosen in order to examine the properties of the scheme. In

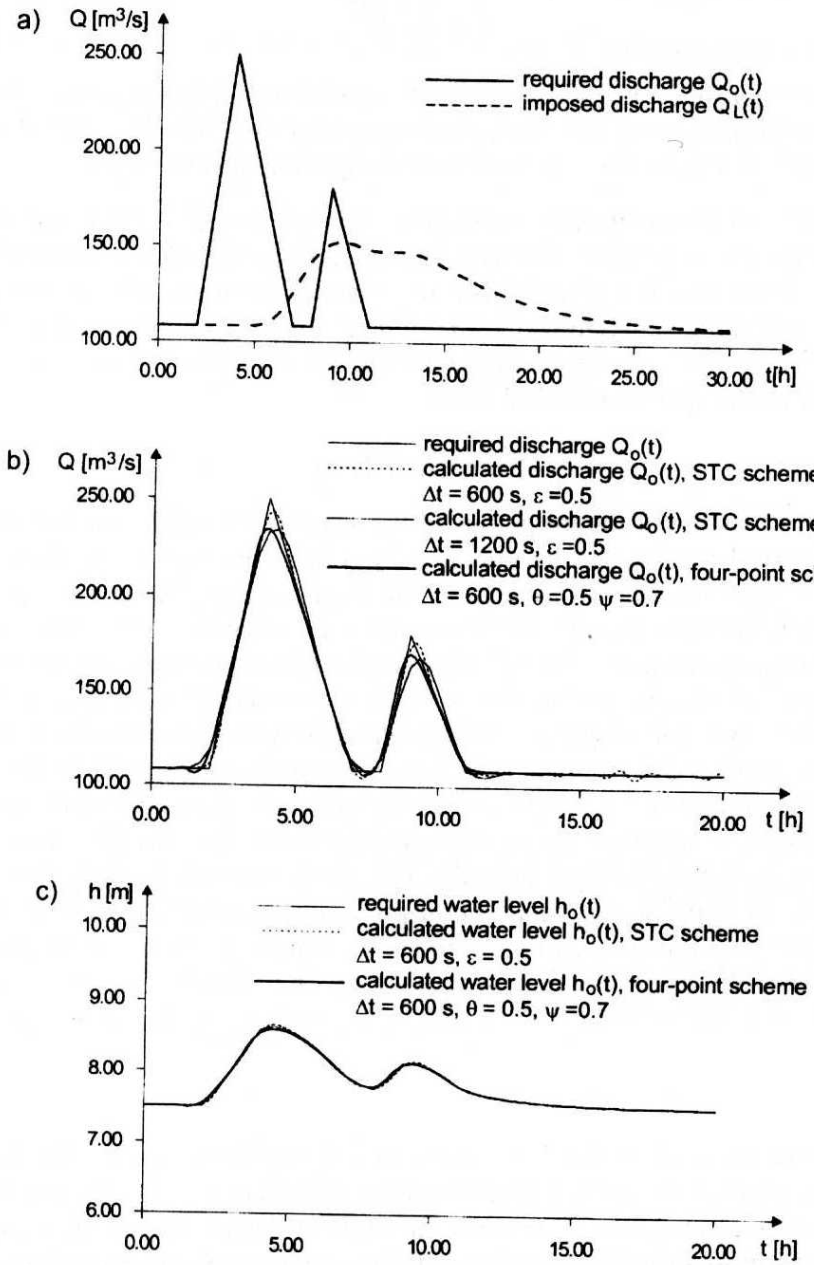

Fig. 6. Comparison of the imposed and computed solutions of the reverse flow routing problem (test 1): a) required discharge $Q_o(t)$ at $x = 0$ and imposed discharge $Q_L(t)$ at $x = L$, b) discharge functions calculated with four-point scheme and STC scheme, c) imposed and calculated water level

the downstream cross-section, the constant water stage is prescribed. The water depth is constant and the downstream condition is $H_L(t) = 2.5$ m. The values of discharge function calculated in the direct problem, both with downstream water stage condition were imposed as the conditions in the inverse problem. The imposed discharge function in downstream cross-section is shown in Fig. 6a. The initial and final boundary conditions on the boundaries $t = 0$ and $t = t_{max} = 48$ h are prescribed as the steady flow condition $Q = 108.038$ m^3/s.

The inverse problem was solved with finite difference implicit four-point and STC schemes. Comparisons of the best results obtained from each of the methods, are presented in Fig. 6b. In the case of the four-point scheme the best results were achieved when $\theta = 0.5$, $\psi = 0.7$, $\Delta t = 600$ s. The Courant's number, defined as

$$Cr = \frac{(U + \sqrt{gH})\Delta t}{\Delta x}, \tag{44}$$

in this case took the values from the range $\langle 3.5 \div 4.3 \rangle$. The solution suffers from the numerical diffusion error, which manifests itself in considerable smoothing of the calculated discharge function. By applying other values of θ and ψ the results not only become worse, but also in some cases the computations fail due to loss of numerical stability.

The results of the calculations confirmed that in the case of properly chosen parameters, the numerical dissipation generated by the STC scheme is considerably less (Fig. 6b). In consequence, the solution is much closer to that desired. The smaller numerical dissipation error enables good matching of the peaks. However, it happens at the cost of quality of results of the steady flow for $t > 12$ h, where the numerical dispersion error causes non-physical oscillations. The results presented were obtained for $\varepsilon = 0.5$ and $\Delta t = 600$ s, $C_r = \langle 3.5 \div 4.4 \rangle$. By increasing the time interval Δt and changing the value of ε, the magnitude of the numerical dissipation and dispersion errors may be influenced. The reduction of the oscillations for steady flow is possible, but at the cost of smoothing the upstream discharge function ($\varepsilon = 0.5$, $\Delta t = 1200$ s, $C_r = \langle 7.0 \div 8.7 \rangle$. However, where determination of the wave culmination is essential, the application of the STC scheme, despite its conditional stability, related parameter value and grid size limitations, leads to results of higher accuracy than in the case of the four-point scheme. The second one is less sensitive to the changes of Δt, but in practice, it always generates numerical diffusion that smoothes the solution and underrates the Q values to a higher degree than the STC scheme. Both methods ensure good mass conservation. The error is no more than 0.005%.

Test 2

If smooth functions are imposed instead of the strict condition given in Test 1, the results of the application of the STC method are even better. The following test is carried out as in Test 1. The rectangular channel of $L = 50$ km, constant

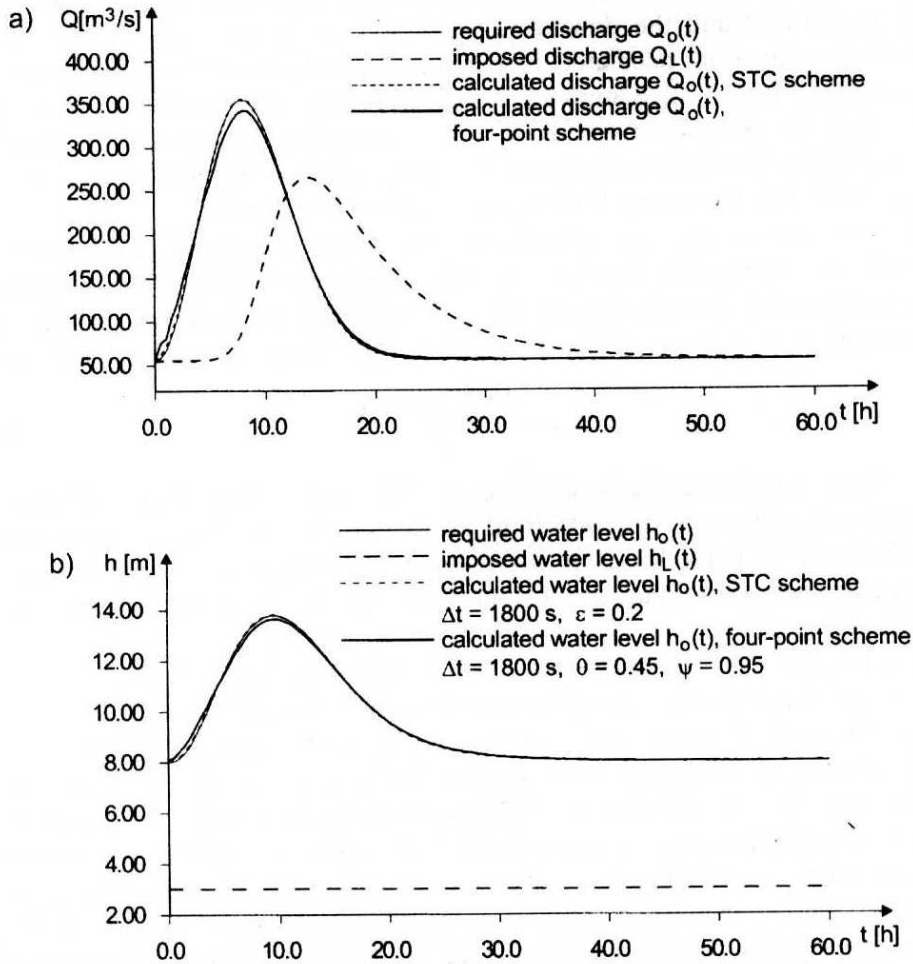

Fig. 7. Comparison of imposed and computed solutions of the reverse flow routing problem (test 1): a) discharge functions $Q(t)$ for $M = 51$ ($\Delta x = 1000$ m), b) water level $h(t)$ for $M = 51$ ($\Delta x = 1000$ m)

bottom slope $S_o = 0.0001$, width $B = 30$ m and Manning coefficient $n = 0.03$ is considered. In steady state the depth in the channel is $H = 3.0$ m and the discharge is $Q = 55.260$ m^3/s. The required discharge function in upstream cross-section is shown in Fig. 7a. Its shape is described by a smooth function

$$Q(t) = Q_o + (Q_m - Q_o)\left[\frac{t - t_p}{T_u}\right]^2 \; exp\left[1 - \left(\frac{t - t_p}{T_u}\right)^2\right], \qquad (45)$$

where $Q_o = 55.260$ m^3/s, $Q_m = 244.740$ m^3/s, $t_p = 0$, $T_u = 28800$ s $= 8$ h. The solution of the direct problem which was also the downstream condition in the inverse problem is also shown in Fig. 7a. The second condition in the downstream

cross-section was $h(t) = H(t) = 3.0$ m = const. The steady flow conditions $Q(x) = 55.260$ m^3/s were imposed on the boundaries $t = 0$ and $t = t_{max} = 100$ h. The distance interval $\Delta x = 1000$ m ($M = 51$) was assumed.

The results of the computations are shown in Fig. 7a. The best results in the case of the four-point scheme were obtained for $\Delta t = 1800$ s, $\theta = 0.45$, $\psi = 0.95$, $C_r = \langle 10.8 \div 18.9 \rangle$; in case of the STC scheme – for $\varepsilon = 0.2$, $\Delta t = 1800$ s, $C_r = \langle 10.8 \div 19.0 \rangle$. Also in this test the solution achieved with four-point scheme suffers from higher numerical errors while the solution obtained with the STC scheme is of very good quality (Fig. 7a, b).

In the next phase of the experiment, the grid size was changed and the distance interval $\Delta x = 500$ m was assumed. In the case of the STC scheme, for $\varepsilon = 0.5$, $\Delta t = 1800$ s, $C_r = \langle 21.7 \div 38.1 \rangle$ the results were of identical quality as in Fig. 7a,b. When the problem is solved with the four-point scheme, many difficulties arise during the obtaining of the solition. In spite of checking many combinations of the values of θ, ψ and Δt, the calculations failed because of the severe numerical errors and no reasonable solution was obtained. It may be stated that the choice of the values of θ and ψ in inverse problem is not easy, which was proved by the tests presented.

6. Final Remarks and Conclusions

The problem of reverse flow routing (RFR) and main difficulties arising during the obtaining of its solution were studied. The main problem, apart from satisfying the conditions of its proper formulation, is the choice of the effective solution algorithm, as in the case of commonly used methods, considerable numerical errors are often observed. As the result, the solution is smoothed or suffers from unphysical oscillations. The Space-Time Conservation (STC) Method applied to the RFR problem was considered in the paper and the stability and accuracy analysis were developed. The proposed method can be successfully applied to the RFR problem, especially in cases where the commonly used schemes fail to produce solution of satisfactory quality. The most important features of the STC scheme, which make the method efficient and attractive, are global and local mass conservation and small dissipation and dispersion errors. In addition the distinguishing features of the STC scheme are space and time unification and relatively simple approximation formulas. The properties of the scheme afford discharge function of a considerable accuracy to be obtained in the upstream cross-section.

Comparison of the results obtained with the STC and the four-point implicit differential schemes confirm that numerical errors produced by the former are considerably smaller. It enables good matching of the peaks of the discharge function, which is of considerable importance.

The STC scheme also affords satisfactory results in the cases in which the friction in the channel is not negligible. The examples presented in literature (Szymkiewicz 1992) and in this paper prove that a satisfactory solution can be also achieved when the Manning coefficient is of considerable value ($n = 0.03$). The remarks of Cunge et al. (1980) concerning the limitations of the channel length also seem too strict. It is obvious, that the accuracy increases in the case of shorter channels. Nevertheless, in the case of a considerable number of channel cross-sections it is also possible to obtain good results. Relatively severe requirements concerning domain boundaries (Test 1) do not cause failure in calculations either. The results are obviously worse than in the case of smooth functions, but in spite of this, the quality of the solution is also satisfactory.

Good properties of the numerical scheme presented in the paper and satisfactory results of the tests proved the effectiveness of the method, which anables successful solving of the RFR problem.

References

Chang S. C. (1995), The Method of Space – Time Conservation Element and Solution Element – A New Approach for Solving the Navier Stokes and Euler Equations, *Journal of Computational Physics*, 119, 295–324.

Cunge J. A., Holly F. M. Jr., Verwey A. (1980), *Practical Aspects of Computational River Hydraulics*, Pitman Publishing Limited, Vol. 3, London.

Dziubiński I., Świątkowski T. (1985), *Handbook of Mathematics* (in Polish), Warszawa, PWN.

Eli R. N., Wiggert J. M., Contractor D. N. (1974), Reverse Flow Routing by the Implicit Method, *Water Resources Research*, 10(3), 597–600.

Fletcher C. A. J. (1991), *Computational Techniques for Fluid Dynamics*, Berlin–Heidelberg, Springer-Verlag, Vol. 1.

Godunow C. K. (1975), *Mathematical Physics Equations* (in Polish), Warszawa, WN–T.

Molls T., Molls F. (1998), Space – Time Conservation Method Applied to Saint-Venant Equations, *Journal of Hydraulic Engineering*, Vol. 124, No. 5, 501–508.

Peyret R., Taylor T. D. (1983), *Computational Methods for Fluid Flow*, New York: Springer-Verlag Inc.

Potter D. (1977), *Computational Physics* (in Polish), Warszawa, PWN .

Szydłowski M. (1998), *Numerical simulation of the Free Surface Rapidly Varied Flow with Discontinuities* (PhD thesis, in Polish), Technical University of Gdańsk.

Szymkiewicz R. (2000), *Mathematical modeling of the Flow in Rivers and Channels* (in Polish), Warszawa, Wydawnictwo Naukowe PWN.

Szymkiewicz R. (1996), Numerical Stability of Implicit Four–Point Scheme Applied to Inverse Linear Flow Routing, *Journal of Hydrology*, 176, 13–23.

Szymkiewicz R. (1993), Solution of the Inverse Problem for the Saint-Venant Equations, *Journal of Hydrology*, 147, 105–120.

Weinerowska K. (2001), *Inverse Problems in Open Channel Hydraulics* (PhD thesis, in Polish), Technical University of Gdańsk.